This is an *Accepted Manuscript*, which has been through the Royal Society of Chemistry peer review process and has been accepted for publication.

Accepted Manuscripts are published online shortly after acceptance, before technical editing, formatting and proof reading. Using this free service, authors can make their results available to the community, in citable form, before we publish the edited article. We will replace this *Accepted Manuscript* with the edited and formatted *Advance Article* as soon as it is available.

You can find more information about *Accepted Manuscripts* in the **Information for Authors**.

Please note that technical editing may introduce minor changes to the text and/or graphics, which may alter content. The journal's standard **Terms & Conditions** and the **Ethical guidelines** still apply. In no event shall the Royal Society of Chemistry be held responsible for any errors or omissions in this *Accepted Manuscript* or any consequences arising from the use of any information it contains.

Journal Name

ARTICLE

Relationship between Activation Energy and Pre-exponential Factor Normalized by Number of Brønsted Acid Sites in Cracking of Short Chain Alkanes on Zeolites

Naonobu Katada,[a] Satoko Sota,[a] Nami Morishita,[a] Kazu Okumura,[b] and Miki Niwa[c]

Reaction rates of C3 to C8 linear and C4 and C5 monomethyl-branched alkanes catalysed by various zeolites (FAU, *BEA, MFI and MOR) were analysed. The pre-exponential factor, normalized with the number of Brønsted acid sites, showed compensatory change of the activation energy. The lower activation energy gave the lower pre-exponential factor, indicating the compensation effect between the activation energy and entropy. The relationship between the pre-exponential factor and activation energy was common in the reaction of butane, pentane, hexane, octane and 2-methylbutane over various catalysts, while propane and 2-methylpropane had pre-exponential factor lower than those observed in the reactions of other alkanes.

Introduction

Alkane cracking is an industrially important reaction. Various aluminosilicates, i.e., natural clay, amorphous silica-alumina, and modified X and Y zeolites with the FAU structure have been applied to this reaction. Ultrastable Y (USY) zeolite and its derivatives have been finally developed until 1960's.[1] Then ZSM-5 zeolite with the MFI structure was added in order to improve the selectivity of branched alkanes in gasoline fraction in 1960-70's.[2] The fundamental components of catalyst have been fixed in these periods.

Kinetic analysis of catalytic cracking of alkane has been carried out. Olson, Haag and Lago found dependence of the reaction rate on the aluminium concentration over a series of ZSM-5 zeolites.[3] Subsequently, dependence of the apparent activation energy (hereafter E_a, in the unit of J mol^{-1}) on the physical adsorption heat throughout different alkanes and zeolite catalysts was found.[4-7] Because of the importance of E_a for controlling the reaction rate, the relationship between E_a and properties of the reactant alkanes and catalyst species has been investigated from different viewpoints. For example, the relationship between E_a and the strength of Brønsted acid sites has been studied.[8-11]

Besides the discussion on the origin of difference in E_a, the compensation effect between E_a and pre-exponential factor A (1) was found on a series of alkanes and zeolite catalysts.[4]

$$E_a = a + b \ln A \qquad (1)$$

where a and b were the constants, and A was defined by Arrhenius equation (2).

$$k' = A e^{-\frac{E_s}{RT}} \qquad (2)$$

where k', A, R and T mean the rate constant in fixed-bed flow reaction (mol s^{-1} kg^{-1}), pre-exponential factor (mol s^{-1} kg^{-1}), gas constant (8.3145 J K^{-1} mol^{-1}) and reaction temperature (K), respectively.

The compensation effect is believed to be due to the compensation between the activation entropy $\Delta S^{*\circ}$ (J K^{-1} mol^{-1}) and activation enthalpy $\Delta H^{*\circ}$ (J mol^{-1}) (3).[12]

$$\Delta H^{*\circ} = c + d \Delta S^{*\circ} \qquad (3)$$

The importance of $\Delta S^{*\circ}$ for determining the catalytic activity of alkane cracking has been pointed out.[13-16]

Corma et al. found that a series of solid acid-catalysed reactions had the compensation effect between A and E_a. The effect was found in heptane cracking, Knoevenagel condensation of benzaldehyde and cyanoacetate, meta-xylene isomerization / transalkylation, cumene (2-phenylpropane) cracking and ortho-xylene isomerization over FAU zeolites with different compositions.[17]

The factors affecting A and E_a and the intrinsic origin of compensation have been discussed for a long time in the field of heterogeneous catalysis.[18] Both of E_a and A have contributions of adsorption and intrinsic activation steps, adding complexity to the analysis. Besides this problem, the pre-exponential factor A is usually calculated based on the rate per weight of catalyst as above, but employing the rate per number of active sites, i.e., turnover frequency, for calculating

the pre-exponential factor must improve the accuracy of analysis. [19] Therefore, in kinetic analysis of such a typical Brønsted acid-catalysed reaction as alkane cracking, the number of Brønsted acid sites is necessary to be considered, but it has been difficult to precisely measure the number of Brønsted acid sites on a solid. Niwa et al. have developed a method of ammonia infrared-mass spectroscopy (IRMS)-temperature-programmed desorption (TPD) to measure the number and strength of each of Brønsted and Lewis acid sites. [20] This was applied in this study, and the pre-exponential factor A was normalized by the measured number of Brønsted acid sites. Thus, kinetic parameters over various (linear C3 to C8 and monomethyl-branched C4 and C5) alkanes were measured using zeolite catalysts with various structures, compositions and

Brønsted acid strengths. Similarity and difference in feature of reactivity of these alkanes throughout catalysts will be clarified.

Experimental

Table 1 lists the catalysts employed in this study and their origins. The acidic zeolites with FAU, BEA, MFI and MOR structures were employed, as well as the USY (FAU) zeolites modified with various extra-framework cations. The number (A_0, mol kg^{-1}) and strength (shown by enthalpy of ammonia desorption ΔH_{NH3}, J mol^{-1}) of Brønsted acid sites were measured by means of the ammonia IRMS-TPD method as described elsewhere. [20]

Table 1 Employed catalysts

Catalyst	Description	A_0 / mol kg^{-1}	ΔH_{NH3} / kJ mol^{-1}	Ref.
H-Y (2.6)*	FAU, [Si]/[Al] = 2.6, ion-exchanged from Na-Y**	1.15	109±9	21
CaH-Y*	FAU, 2[Ca]/[Al] = 0.37, ion-exchanged from NH$_4$-Y	0.50	122±6	22
BaH-Y*	FAU, 2[Ba]/[Al] = 0.35, ion-exchanged from NH$_4$-Y	0.74	118±5	22
E-USY*	FAU, NH$_4$-Y steamed at 823 K and treated with Na$_2$H$_2$-ethylenediaminetetraacetic acid	0.47	137±7	23
N(0.5)-USY*	FAU, NH$_4$-Y steamed at 823 K and treated with 0.5 mol dm^{-3} NH$_4$NO$_3$	0.16	157±10	24
N(2.3)-USY*	FAU, NH$_4$-Y steamed at 823 K and treated with 2.3 mol dm^{-3} NH$_4$NO$_3$	0.22	153±10	24
N(7.5)- USY*	FAU, NH$_4$-Y steamed at 823 K and treated with 7.5 mol dm^{-3} NH$_4$NO$_3$	0.27	146±11	24
S-USY*	FAU, NH$_4$-Y steamed at 823 K and treated with 0.5 mol dm^{-3} (NH$_4$)$_2$SO$_4$	0.24	156±10	24
C-USY*	FAU, NH$_4$-Y steamed at 823 K and treated with 0.5 mol dm^{-3} CH$_3$COONH$_4$	0.21	154±10	24
H-β (13)	*BEA, [Si]/[Al] = 13, PQ Corp.,	0.35	129±12	****
H-β (75)	*BEA, [Si]/[Al] = 75, JRC-Z-HB150 (1)***	0.12	135±5	****
NaH-M (7.5)*	MOR, NaH-mordenite, [Si]/[Al] = 7.5, [Na]/[Al] = 0.07, ion-exchanged from JRC-Z-M15***	0.15	142±7	20
H-ZSM-5 (12)	MFI, [Si]/[Al] = 12, Tosoh Corp.	0.81	132±9	****
H-ZSM-5 (20)*	MFI, [Si]/[Al] = 20, Synthesized	0.68	126±6	****
H-ZSM-5 (35)*	MFI, [Si]/[Al] = 35, Synthesized	0.45	129±3	****
H-ZSM-5 (45)	MFI, [Si]/[Al] = 45, JRC-Z5-90H (1)***	0.15	141±6	****
H-ZSM-5(62)*	MFI, [Si]/[Al] = 62, Synthesized	0.20	128±1	****
H-ZSM-5 (126)*	MFI, [Si]/[Al] = 126, Synthesized	0.09	137±2	****

*: Stored as NH$_4$ form, and converted into H form in the pre-treatment of ammonia IRMS-TPD measurements and catalytic tests.

**: Na-Y was kindly supplied by Catalysts & Chemicals Industries Co. Ltd.

***: Reference catalyst obtained from Catalysis Society of Japan

****: Present study.

The catalytic tests were carried out at relatively high reaction temperatures and low alkane pressures where Haag-Dessau mechanism is believed to be predominant,[25] as follows. The reaction was performed in a fixed-bed reactor in a flow of helium carrier gas at 753 - 813 K and atmospheric pressure. The nomenclature and partial pressures at the inlet of reactor (initial pressure P_0, Pa) of reactant alkanes are listed in Table 2. In most cases the reaction rate was constant without catalyst degradation at least for 4 h of the time on stream, and the averaged value during 4 h was adopted in the following analysis. Deactivation of catalyst during 4 h of the time on stream was observed on some samples of USY zeolites. The values at 15 min of the time on stream were adopted in these cases, and the fresh catalyst was used for each run. The W (catalyst weight, kg) / F_m (reactant flow rate, mol s^{-1}) ratio was adjusted to keep conversion < 10 %. Here the first-order reaction is assumed, because the reaction rate was approximately proportional to the pressure of alkane in preliminary experiments employing some of catalysts and alkanes. Some examples of pressure-dependence of reaction rate have been published.[26,27]

$$r = -\frac{d\left(\dfrac{P}{P°}\right)}{d\left(\dfrac{W}{F_m}\right)} = k'\left(\frac{P}{P°}\right) \qquad (4)$$

where r, P and $P°$ are the reaction rate (mol s^{-1} kg^{-1}), partial pressure of alkane (Pa) and pressure of standard conditions (10^5 Pa), respectively. Hence, k' was estimated by the following equation from the conversion x experimentally measured.

$$k' = \frac{F_m P°}{WP_0}\ln\frac{1}{1-x} \qquad (5)$$

It should be noted that x in (5) shows the total conversion of alkane, which covers not only cracking but also such reactions as isomerization and dehydrogenation in the present study.

Table 2 Nomenclatures and initial pressures of alkanes

Alkane	P_0 / Pa
nC3 (propane)	1.0×10^4
nC4 (butane)	1.0×10^4
nC5 (pentane)	1.2×10^4
nC6 (hexane)	6.0×10^3
nC8 (octane)	1.9×10^4
iC4 (2-mthylpropane)	1.0×10^4
iC5 (2-methylbutane)	1.2×10^4

Results and Discussion

From the Arrhenius plots (some examples are shown in Figure 1), E_a and A were calculated and listed in Table 3. As discussed in our previous papers,[10,11] reasonable relationships between E_a and desorption enthalpy of ammonia were observed on most catalysts (Figure S1), but some exceptional behaviours were observed as follows. (1) In the reaction of short alkane (propane), MFI with relatively low [Al] showed E_a predicted along the relationship between E_a and ammonia desorption enthalpy, while samples with high [Al] showed exceptionally low E_a. (2) In the reaction of long alkane (hexane and octane), MFI with low [Al] and MOR showed exceptionally high E_a. MFI has smaller micropores (10-ring) than other zeolites employed in this study. MOR has large 12-ring channels but they are one-dimensional inducing low diffusion behaviour of large molecules. The exceptional behaviours are probably related with these features in pore structures, but it has been difficult to explain the reason. On the other hand, so-called intrinsic activation energy [(apparent activation energy)-(enthalpy of alkane adsorption)] was approximately constant on most catalysts as stated.[4-7] Apart from these behaviours of E_a, we will focus on the relationship between A and E_a in the present study.
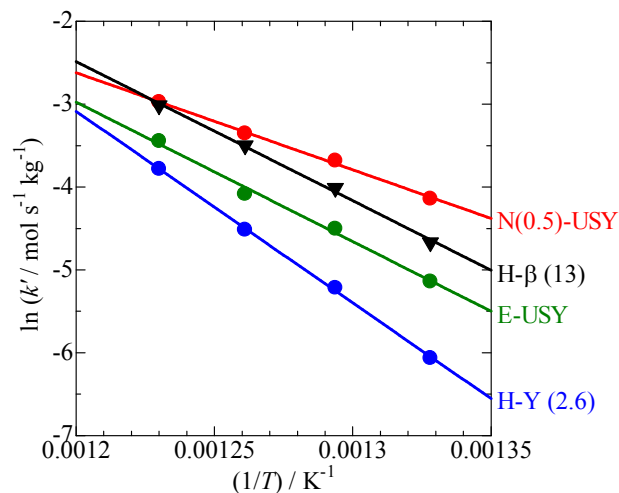

Figure 1. Examples of Arrhenius plot in the reaction of nC4 (butane).

Table 3 Activation energy and pre-exponential factor

Catalyst	E_a / kJ mol^{-1}							A / mol s^{-1} kg^{-1}						
	nC3	nC4	nC5	nC6	nC8	iC4	iC5	nC3	nC4	nC5	nC6	nC8	iC4	iC5
H-Y (2.6)	223	192	166	130	124	180	150	1.2×10^{11}	5.1×10^{10}	1.5×10^9	1.3×10^7	3.5×10^6	2.9×10^9	2.0×10^8
CaH-Y	174	170	140	122	98	148	121	3.9×10^8	1.1×10^9	7.8×10^7	1.1×10^7	1.7×10^5	2.5×10^7	2.4×10^6
BaH-Y	202	-	154	123	120	-	-	1.0×10^{10}	-	3.8×10^8	5.6×10^6	2.4×10^6	-	-
E-USY	162	140	-	-	-	118	106	7.3×10^{07}	3.0×10^7	-	-	-	5.1×10^5	1.4×10^6
N(0.5)-USY	104	97	93	63	43	88	78	1.9×10^4	9.3×10^4	1.1×10^5	6.5×10^3	1.3×10^3	1.5×10^4	4.0×10^4
N(2.3)-USY	-	-	-	69	51	-	-	-	-	-	2.0×10^4	4.1×10^3	-	-
N(7.5)- USY	-	-	-	77	55	-	-	-	-	-	6.3×10^4	7.1×10^3	-	-
S-USY	116	104	-	81	43	97	-	8.7×10^4	2.8×10^5	-	5.7×10^4	1.3×10^3	2.3×10^4	-
C-USY	127	101	-	71	55	87	70	3.8×10^5	1.6×10^5	-	2.7×10^4	7.1×10^3	9.7×10^3	6.9×10^3
H-β (13)	165	140	-	107	82	-	-	8.1×10^7	4.7×10^7	-	3.2×10^6	6.5×10^4	-	-
H-β (75)	173	-	-	-	-	-	-	6.6×10^7	-	-	-	-	-	-
NaH-M (7.5)	153	-	-	78	94	-	-	3.2×10^7	-	-	4.5×10^3	4.1×10^4	-	-
H-ZSM-5 (12)	141	-	-	102	-	-	-	1.8×10^7	-	-	2.7×10^6	-	-	-
H-ZSM-5 (20)	-	126	109	93	76	-	-	-	8.6×10^6	2.3×10^6	5.1×10^5	1.9×10^5	-	-
H-ZSM-5 (35)	149	-	-	116	-	-	-	2.7×10^7	-	-	4.5×10^6	-	-	-
H-ZSM-5 (45)	156	142	132	120	102	-	-	1.3×10^7	-	-	5.6×10^6	-	-	-
H-ZSM-5 (62)	159	-	-	121	-	-	-	1.3×10^7	3.2×10^7	1.2×10^7	5.0×10^6	1.0×10^6	-	-
H-ZSM-5 (126)	164	-	-	126	-	-	-	2.7×10^7	-	-	9.2×10^6	-	-	-

Figure 2 shows plots of A divided by the number of Brønsted acid sites against E_a. Thus normalised pre-exponential factors (A/A_0 in the unit of s^{-1}) of nC4-nC8 and iC5 (filled symbols in Figure 2) showed a common relationship against E_a over all the employed catalysts. The higher E_a gave the higher A/A_0, indicating that the pre-exponential factor tends to compensate the change of activation energy.
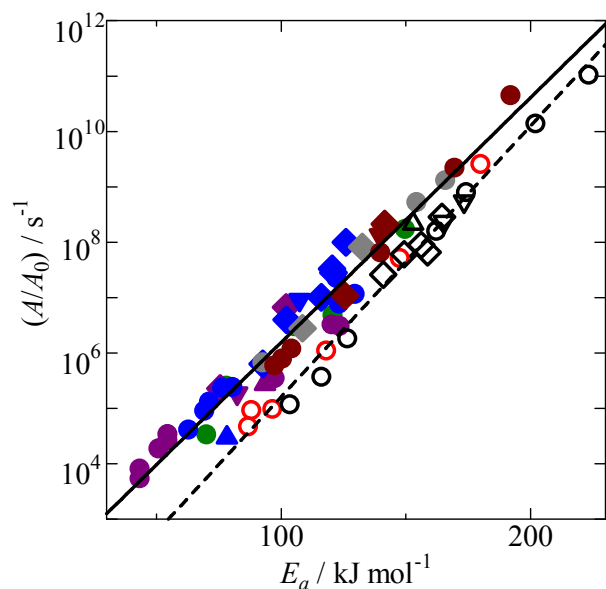
Figure 2. Plots of A/A_0 against E_a of the reactions of nC3 (black, opened), iC4 (red, opened), nC4 (brown, filled), iC5 (green, filled), nC5 (grey, filled), nC6 (brown, filled) and nC8 (purple, filled) over FAU (●), BEA (▼), MFI (◆) and MOR (▲) zeolites. The solid lines is the linear relationships determined by minimum square method for the results of nC4-nC8 and iC5 reactions, whereas the dotted line is that for nC3 and iC4.

The pre-exponential factors of nC3 and iC4 (open symbols) also showed a relationship where the higher E_a gave the higher A/A_0. However, the values of A/A_0 in the nC3 and iC4 reactions were obviously lower than those observed at the same E_a in the reactions of nC4-nC8 and iC5 alkanes. In other words, alkanes having carbon chains equal to or longer than C4 showed high activation energy at the same pre-exponential factor. This suggests a difference in the reaction mechanism among these alkanes.

Then we calculate the activation enthalpy and entropy according to Eyring's equation.[28]

$$\frac{h_P k}{\kappa k_B T} = e^{\frac{\Delta S^{*\circ}}{R}} e^{-\frac{\Delta H^{*\circ}}{RT}}$$

(6)

where h_P, k, κ, k_B, $\Delta S^{*\circ}$ and $\Delta H^{*\circ}$ are Planck constant (6.63×10^{-34} J s), rate constant in absolute kinetics (s^{-1}), transmission coefficient, Boltzmann constant (1.38×10^{23} J K^{-1}), standard entropy of activation (J K^{-1} mol^{-1}) and standard enthalpy of activation (J mol^{-1}). Here we assumed $\kappa = 1$ and $k = \frac{k'}{A_0}$; the latter assumption is equivalent to that the analysis was based on the turnover frequency (reaction rate per number of active sites). From the slope and intercept of plot of $\ln \frac{k}{T}$ against $\frac{1}{T}$, $\Delta S^{*\circ}$ and $\Delta H^{*\circ}$ were obtained according to the equation (7). Some examples of the plot are shown in Figure 3. It is noteworthy that thus obtained $\Delta S^{*\circ}$ includes entropy change of the alkane molecule from the gaseous state at

10^5 Pa to the adsorbed state, because the rate constant normalized by $\left(\frac{P}{P^\circ}\right)$ was used.

$$\ln \frac{k}{T} = -\frac{\Delta H^{*\circ}}{R}\frac{1}{T} + \ln\frac{\kappa k_B}{h_P} + \frac{\Delta S^{*\circ}}{R}$$
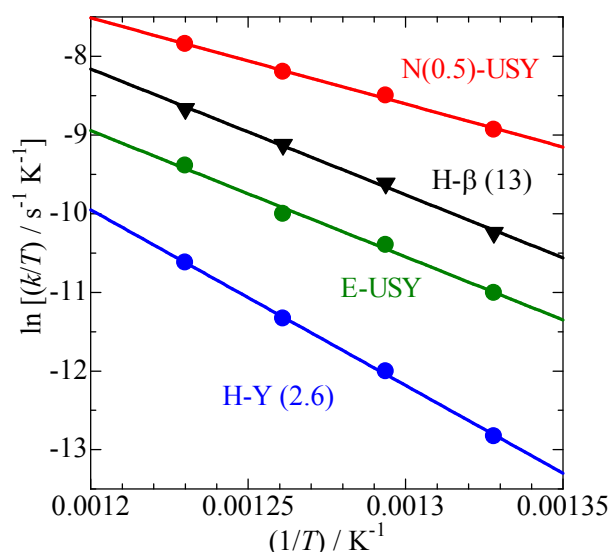
(7)

Figure 3. Examples of Eyring plot in the reaction of nC4 (butane).

Figure 4 indicates a linear relationship between $\Delta S^{*\circ}$ and $\Delta H^{*\circ}$ in the reactions of nC4-nC8 and iC5 over all the employed catalysts, whereas a different linear relationship exists in the reactions of nC3 and iC4.
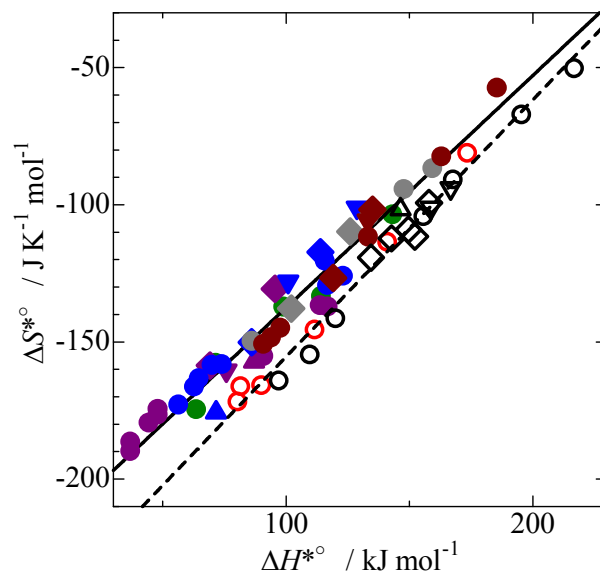
Figure 4. Plots of $\Delta S^{*\circ}$ against $\Delta H^{*\circ}$ of the reactions of nC3 (black, opened), iC4 (red, opened), nC4 (brown, filled), iC5 (green, filled), nC5 (grey, filled), nC6 (blue, filled) and nC8 (purple, filled) over FAU (●), BEA (▼), MFI (◆) and MOR (▲) zeolites. The solid lines is the linear relationships determined by minimum square method for the results of nC4-nC8 and iC5 reactions, whereas the dotted line is that for nC3 and iC4.

The changes in enthalpy and entropy during the reaction can be drawn as shown in Figure 5. The positive values of $\Delta H^{*\circ}$ indicate that the enthalpy of transition state is higher than that of reactant, whereas the negative values of $\Delta S^{*\circ}$ indicate that the entropy of transition state is lower. The latter is due to the loss of freedom by the adsorption of molecule on the active centre. The compensatory correlation between $\Delta S^{*\circ}$ and $\Delta H^{*\circ}$ tells us that the active centre which gives a lower activation enthalpy forms an intermediate ($AH^{+}{\cdot}{\cdot}Zs^{-}$ in Figure 5) with lower entropy than the intermediate on the centre with higher activation enthalpy ($AH^{+}{\cdots}Zw^{-}$). The compensation between $\Delta S^{*\circ}$ and $\Delta H^{*\circ}$ is generally observed in various non-catalytic and catalytic reactions including solid acid-catalysed reactions.[12,16,29-33] It is speculated that the stronger bonding of intermediate to the active centre more significantly reduces the extent of freedom, resulting in the lower entropy.[29,34] Also in the activation of alkanes on zeolites, it is speculated that the freedom of movement of $AH^{+}{\cdot}{\cdot}Zs^{-}$ is smaller than that of $AH^{+}{\cdots}Zw^{-}$, because the former is more tightly bound by the solid surface. Quantum chemical calculations have indicated that the activation entropy is dependent on the structure of intermediate in the reaction of propane on an acid site.[35] This supports our postulation.
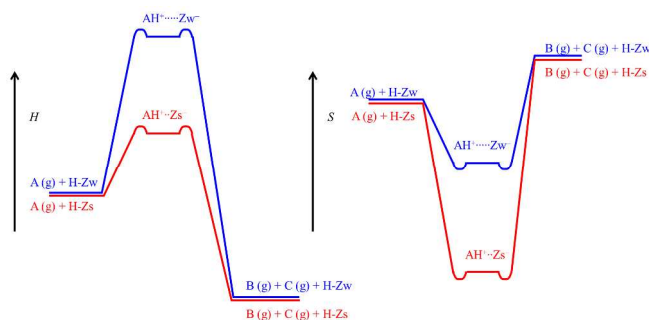

Figure 5. Diagram of enthalpy (left) and entropy (right) changes in cracking reaction. A (g) shows the reactant alkane in the gas phase, while B (g) and C (g) show the products. HZs shows the proton form zeolite which gives low activation enthalpy, whereas HZw means the zeolite which gives high activation enthalpy. The transition states on HZs and HZw are shown here as $AH^{+}{\cdot}{\cdot}Zs^{-}$ and $AH^{+}{\cdots}Zw^{-}$, respectively.

It is speculated that alkanium cation type A shown in Figure 6 is more stable than type B. An alkane with a chain equal to or longer than C4 can make the type A. In the reaction of such a molecule, the route via type A should be the predominant mechanism. On the other hand, the linear C3 and branched C4 can form only type B. The observed difference in the relationships between $\Delta S^{*\circ}$ and $\Delta H^{*\circ}$ indicates different thermodynamic behaviours of reaction mechanisms via these intermediates.
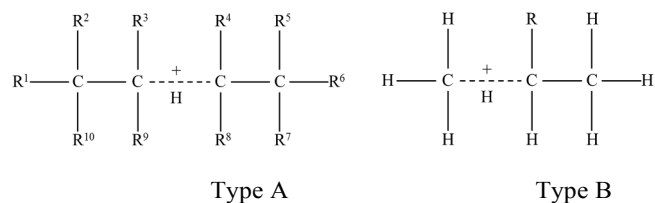

Figure 6. Different types of alkanium cation. R^{n} or R can be alkyl group or H.

Conclusions

The pre-exponential factor normalized by the number of Brønsted acid sites was related with the activation energy in the reactions of C3-C8 alkanes over various zeolites. A compensation effect in which the lower the activation energy, the lower the pre-exponential factor, corresponding to the lower entropy of activation, was observed. A common relationship between the activation energy and pre-exponential factor was observed for linear C4-C8 alkanes and 2-methylbutane, while a different relationship was observed for propane and 2-methylpropane, suggesting different reaction mechanisms.

Acknowledgement

Notes and references

[a] Department of Chemistry and Biotechnology, Graduate School of Engineering, Tottori University, 4-101 Koyama-cho Minami, Tottori 680-8552, Japan.

[b] Department of Applied Chemistry, Faculty of Engineering, Kogakuin University, 2665-1 Nakano, Hachioji, Tokyo 192-0015, Japan.

[c] Department of Research, Nagoya Industrial Science Research Institute, 2F, Noah Yotsuya Build., 1-13 Yotsuya-dori, Chikusa-ku, Nagoya 464-0819, Japan.

1   I. E. Maxwell and W. H. J. Stork, *Stud. Surf. Sci. Catal.*, 2001, **137**, 747.

2   J. Scherzer, *Catal. Rev. -Sci. Eng.*, 1989, **31**, 215.

3   D. H. Olson, W. O. Haag and R. M. Lago, *J. Catal.*, 1980, **61**, 390.

4   W. O. Haag, *Stud. Surf. Sci. Catal.*, 1994, **84**, 1375.

5   S. Kotrel, M. P. Rosynek and J. H. Lunsford, *J. Phys. Chem., B*, **1999**, 103, 818.

6   S. M. Babitz, B. A. Williams, J. T. Miller, R. Q. Snurr, W. O. Haag and H. H. Kung, *Appl. Catal., A: Gen.*, 1999, **179**, 71.

7   J. A. van Bokhoven, M. Tromp, D. C. Koningsberger, J. T. Miller, J. A. Z. Pieterse, J. A. Lercher, B. A. Williams and H. H. Kung, *J. Catal.*, 2001, **202**, 129.

8   A. Auroux, A. Tuel, J. Bandiera, Y. B. Taarit and J. M. Guil, *Appl. Catal., A: Gen.*, 1993, **93**, 181.

9   P. Borges, R. R. Pinto, M. A. N. D. A. Lemos, F. Lemos, J. C. Védrine, E. G. Deroane and F. R. Ribeiro, *J. Mol. Catal., A: Chem.*, 2005, **229**, 127.

10 N. Katada, K. Suzuki, T. Noda, W. Miyatani, F. Taniguchi and M. Niwa, *Appl. Catal., A: Gen.*, 2010, **373**, 208.

11 M. Niwa, K. Suzuki, N. Morishita, G. Sastre, K. Okumura and N. Katada, *Catal. Sci. Tech.*, 2013, **3**, 1919.

12 J. E. Leffler and E. Grunwald, Rates and Equilibria of Organic Reactions: As Treated by Statistical, Thermodynamic and Extrathermodynamic Methods, Dover Publications, New York, 1989.

13 F. Eder and J. A. Lercher, *Zeolites*, 1997, **18**, 75.

14 F. Eder, M. Stockernhuber and J. A. Lercher, *J. Phys. Chem., B*, **1997**, 101, 5414.

15 T. L. M. Maesen, E. Beerdsen, S. Calero, D. Dubbeldam and B. Smit, *J. Catal.*, 2006, **237**, 278.

16 A. Bhan, R. Gounder, J. Macht and E. Iglesia, *J. Catal.*, 2008, **253**, 221.

17 A. Corma, F. Llopis, J. B. Monton and S. Weller, *J. Catal.*, 1993, **142**, 97.

18 G. C. Bond, *Catal. Today*, 1999, **49**, 41.

19 W. R. Patterson and J. J. Rooney, *J. Catal.*, 1994, **146**, 310.

20 M. Niwa, K. Suzuki, N. Katada, T. Kanougi and T. Atoguchi, *J. Phys. Chem., B*, 2005, **109**, 18749.

21 N. Katada, Y. Kageyama and M. Niwa, *J. Phys. Chem., B*, 2000, **104**, 7561.

22 K. Suzuki, T. Noda, N. Katada and M. Niwa, *J. Catal.*, 2007, **250**, 151.

23 N. Katada, Y. Kageyama, K. Takahara, T. Kanai, H. A. Begum and M. Niwa, *J. Mol. Catal., A: Chem.*, 2004, **211**, 119.

24 K. Okumura, T. Tomiyama, N. Morishita, T. Sanada, K. Kamiguchi, N. Katada and M. Niwa, *Appl. Catal., A: Gen.*, 2011, **405**, 8.

25 W. O. Haag and R. M. Dessau, in: *Proc. 8th Intern. Congr. Catal., Vol. 2*, Varlag-Chemie, Weinheim, 1984, 305.

26 M. Niwa, S. Sota and N. Katada, *Catal. Today*, 2012, **185**, 17.

27 M. Niwa, N. Morishita, H. Tamagawa and N. Katada, *Catal. Today*, 2012, **198**, 12.

28 S. Glasstone, K. J. Leidler and H. Eyring, Theory of Rate Processes, McGraw-Hill, New York, 1941.

29 J. E. Leffer, *J. Org. Chem.*, 1955, **20**, 1202.

30 A. K. Galway, *Adv. Catal.*, 1977, **26**, 247.

31 T. K. Cheung, F. C. Jentoft, J. L. d'Itri, B. C. Gates, *Chem. Eng. Sci.*, 1997, **52,** 4607.

32 D. C. Longstaff, *Energy & Fuels*, 2012, **26**, 801.

33 L.-E. Sandoval-Díaz, J.-M. Martínez-Gil, C. A. Trujillo, *J. Catal.*, 2012, **294**, 89.

34 Y. Inoue, Y. Liu, L.-H. Tong, B.-J. Shen and D.-S. Jin, *J. Am. Chem. Soc.*, 1993, **115**, 10637.

35. T. Bučko, L. Benco, H. Hafner, J. G. Ángyán, *J. Catal.*, 2011, **279**, 220.